Development 133, 4679-4689 (2006) doi:10.1242/dev.02654

The *Arabidopsis elch* mutant reveals functions of an ESCRT component in cytokinesis

Christoph Spitzer[1], Swen Schellmann[1,*], Aneta Sabovljevic[1], Mojgan Shahriari[1], Channa Keshavaiah[1], Nicole Bechtold[2], Michel Herzog[3], Stefan Müller[4], Franz-Georg Hanisch[5] and Martin Hülskamp[1,*]

Recently, an alternative route to the proteasomal protein-degradation pathway was discovered that specifically targets transmembrane proteins marked with a single ubiquitin to the endosomal multivesicular body (MVB) and, subsequently, to the vacuole (yeast) or lysosome (animals), where they are degraded by proteases. Vps23p/TSG101 is a key component of the ESCRT I-III machinery in yeast and animals that recognizes mono-ubiquitylated proteins and sorts them into the MVB. Here, we report that the *Arabidopsis ELCH* (*ELC*) gene encodes a Vps23p/TSG101 homolog, and that homologs of all known ESCRT I-III components are present in the *Arabidopsis* genome. As with its animal and yeast counterparts, ELC binds ubiquitin and localizes to endosomes. Gel-filtration experiments indicate that ELC is a component of a high-molecular-weight complex. Yeast two-hybrid and immunoprecipitation assays showed that ELC interacts with *Arabidopsis* homologs of the ESCRT I complex. The *elc* mutant shows multiple nuclei in various cell types, indicating a role in cytokinesis. Double-mutant analysis with *kaktus* shows that increased ploidy levels do not influence the cytokinesis effect of *elc* mutants, suggesting that *ELC* is only important during the first endoreduplication cycle. Double mutants with *tubulin folding cofactor a* mutants show a synergistic phenotype, suggesting that ELC regulates cytokinesis through the microtubule cytoskeleton.

KEY WORDS: Endosome, ESCRT, Mono-ubiquitylation, Multivesicular body, Protein degradation, *Arabidopsis*

INTRODUCTION

The stability of proteins is tightly controlled to not only destroy non-functional or misfolded proteins, but also to regulate biological processes. The best-analyzed pathway is the proteasomal protein degradation pathway (Hershko, 1983; Vierstra and Callis, 1999). Proteins that are subject to degradation are linked to chains of several ubiquitin molecules by a cascade of E1, E2 and E3 enzymes. Poly-ubiquitin-marked proteins are targeted to the proteasome, a large complex where the protein is degraded.

Recently, an alternative ubiquitin-dependent route for protein degradation was discovered (Babst, 2005; Katzmann et al., 2001). In this pathway, proteins labeled by a single ubiquitin are targeted to the lysosome (animals) or vacuole (yeast) (Babst, 2005). This pathway is also used for the delivery of proteins (e.g. proteases) that normally reside in the vacuole (Babst et al., 2000).

The initial step is the recognition of mono-ubiquitlyated proteins by Vps23p and Vps27p (Bilodeau et al., 2002; Bilodeau et al., 2003). Vps23p is a component of the ESCRT I complex that is located at the late endosome, the multivesicular body (MVB). The MVB contains numerous vesicles that originate from the invagination of the outer membrane. Proteins targeted to the MVB membrane by Vps23p and Vps27p become internalized with the aid of the ESCRT II and ESCRT III complexes (Babst et al., 2002a; Babst et al., 2002b; Katzmann et al., 2001). The MVBs eventually fuse with the vacuole/lysosome where proteins are degraded by luminal proteases (Odorizzi et al., 1998).

This protein degradation pathway appears to specifically recognize proteins linked to a single ubiquitin. This is evident from the finding that pCPS, a precursor of carboxypeptidase S, is misguided to the vacuolar membrane when the N-terminal lysine to which ubiquitin is bound is replaced by other amino acids (Katzmann et al., 2001). Conversely, proteins that are not normally targeted to the vacuole were transported into the vacuole when linked to single ubiquitin molecules (Urbanowski and Piper, 2001). This pathway is also found in mammals. Homologs of all the components of yeast ESCRT complexes have been found, and the human tumor susceptibility gene 101 protein (TSG101) was shown to be the ortholog of Vps23p (Babst, 2005). Individuals deficient in TSG101 develop breast cancer, and mutant cell lines show mitotic defects including aberrant mitotic spindles, multiple nuclei and nuclear anomalies (Xie et al., 1998).

The yeast and plant vacuole and the animal lysosome can be considered functionally similar compartments. All are characterized by an acidic pH and the existence of proteases. Vacuolar protein degradation in plants has been studied in recent years (Vitale and Galili, 2001; Vitale and Raikhel, 1999), but was not linked to the mono-ubiquitin-mediated pathway. In this study, we describe the isolation and functional characterization of the *ELCH* (*ELC*) gene. The *elc* mutant was initially identified because of a trichome morphogenesis phenotype. A closer analysis showed that *elc* mutants have multiple nuclei, not only in trichomes but also in all endoreduplicating cell types analyzed. The *ELC* gene encodes a protein with sequence similarity to yeast Vps23p and human TSG101, which are components of the ESCRT I-III protein sorting machinery. All known components of the ESCRT I-III complexes are found in the *Arabidopsis* genome, indicating that the mono-ubiquitin-dependent vacuolar protein degradation pathway is conserved between plants, yeast and animals. The ELC protein binds

[1]University of Köln, Botanical Institute III, Gyrhofstr. 15, 50931 Köln, Germany. [2]MEDICAGO Inc., 1020, route de l'Église, bureau 600, Sainte-Foy, Québec G1V 3V9, Canada. [3]Laboratoire de Génétique Moléculaire des Plantes, CNRS/Universite J. Fourier BP 53, 38041 Grenoble Cedex 09, France. [4]Centre for Molecular Medicine Cologne and [5]Institute of Biochemistry II, Medical Faculty, University of Cologne, Joseph-Stelzmann-Str. 52, 50931 Köln, Germany.

*Authors for correspondence (e-mail: swen.schellmann@uni-koeln.de; martin.huelskamp@uni-koeln.de)

Accepted 20 September 2006

ubiquitin in vitro. Gel filtration assays suggest that ELC is part of a large protein complex, and yeast two-hybrid and co-immunoprecipitation assays show that ELC binds to *Arabidopsis* VPS37 and VPS28. A YFP:ELC fusion protein is localized to endosomal compartments. We show that *tubulin folding cofactor a* mutants synergistically enhance the phenotype, suggesting that ELC function is linked to microtubules.

MATERIALS AND METHODS

Plant materials and genetic analysis

The *elc* mutant was isolated from a T-DNA-transformed Ws2 ecotype population generated at the INRA, Versailles. The *kaktus* and *stichel* mutants are EMS mutants in a Landsberg *erecta* (L*er*) ecotype. Plants were grown on MS medium (Duchefa, Haarlem, The Netherlands) with 1% glucose under continuous light at 22°C, or in soil under long-day conditions at 24°C.

Constructs and recombinant DNA

The rescue of the *elc* mutant was performed with a fragment amplified from the P1 clone MQC3 using Expand High Fidelity Polymerase (Roche) and the following primers: CS023, 5′-GGGGACAAGTTTGTACAAAAA-AGCAGGCTCAAGCAGGAGTGTCTAGG-3′; and CS038, 5′-GGGG-ACCACTTTGTACAAGAAAGCTGGGTGTTGAGGAATGTATGGGC-3′. The PCR product was gel purified and cloned into the *Ecl*136II restriction site of pCAMBIA-1300 (GenBank accession number AF234296). The 35S::ELC-HA fusion was generated using the following primers: CS063, 5′-AAGGGCCCGTCGACCATGGTTCCCCCGCC-3′; and CS064, 5′-TAGGGCCCGCGGCCGCTCAAGCGTAATCTGGAACATCATATGGG-TACCTACCTGCGATGGCTGC-3′, which includes the sequence of the HA-tag. The PCR product was subcloned into pGEMT®-easy (Promega), excised with *Sal*I and *Not*I, blunt-ended and then ligated into the *Sal*I site of pBinAR (Hofgen and Willmitzer, 1990).

The cDNA for *Arabidopsis* VPS37-1 was obtained from RIKEN Genomic Sciences Centre (Seki et al., 1998; Seki et al., 2002).

Flanking genomic sequences of the T-DNA insertions were isolated using Vectorette PCR. The position of the T-DNA insertion was studied by TAIL-PCR using nested primers annealing within the coding sequence:
AS-TAIL-1, 5′-TTTATGCACAACGATGGTCGCTCCG-3′;
AS-TAIL-2, 5′-CGCACATGTCACTCCTTCTGGTCTCGTT-3′; and
AS-TAIL-3, 5′-AGACCGTTCCCGCCATCACCTTACG-3′.

For the RT-PCR analysis, primers were chosen from regions where the *ELC* gene and its close homolog At5g13860 show significant differences:
AS-ELCHRT-fw1, 5′-ACACCGTTTAACTCCGATGGTTCCCCC-3′;
AS-ELCHRT-rev1, 5′-GGTGGTGAACATGCTGCACTTGCACCC-3′;
AS-ELCHHOMRT-fw, 5′-GTCATCTGTCGTCGTCTTCAAGTAATCG-3′; and
AS-ELCHHOMRT-Rrev, 5′-TGTATATTCCTATACCCAATAAAAATCG-3′.

As neither gene contains introns, an RT reaction without reverse transcriptase was performed as a control for genomic contamination. To calibrate cDNA amounts, actin expression was determined using primers: AS-Act-RT3, 5′-GGATAGCATGTGGAAGTGCATAC-3′; and AS-Act-RT5, 5′-TGCGACAATGGAACTGGAATG-3′.

Ubiquitin binding assay

Crude protein extracts were made from 14-day-old transgenic plants expressing the 35S:ELC-HA construct using a protein extraction buffer (50 mM phosphate, 150 mM NaCl, 5 mM DTT) and Complete Protease Inhibitor (Roche) according to the manufacturer's instructions. Crude extracts were purified by centrifugation at 16 000 ***g*** at 4°C for 5 minutes.

Ubiquitin-agarose beads (Sigma) and Protein G-agarose beads (Roche) were equilibrated in extraction buffer and an equal volume of plant extract was added. After 2 hours at 4°C with slight agitation, the beads were centrifuged at 400 ***g*** and washed two to three times with extraction buffer. Beads and washing fractions were incubated with loading buffer at 99°C for 10 minutes. The proteins were separated by SDS-PAGE and detected by western blotting. The HA epitope was detected with rat anti-HA monoclonal antibody (Roche). An HRP-linked goat anti-rat secondary antibody was used (Jackson Immuno Research Laboratories).

Gel filtration chromatography

Protein extracts were made from plants expressing the ELC-HA construct under control of the CMV 35S promoter. Eight plants were ground at 4°C in 200 μl PC buffer [one tablet of Complete Protease Inhibitor in 2 ml P buffer (50 mM phosphate, 150 mM NaCl, pH 7.0)]. After adding 600 μl P buffer, the homogenate was transferred to 2-ml reaction tubes and centrifuged at 16000 ***g*** for 45 minutes at 4°C. A 50 μl aliquot of this extract was passed immediately over a Superose 6 10/300 GL gel filtration column (Amersham Bioscience). Parameters for the BioLogic DuoFlow workstation (BioRad)

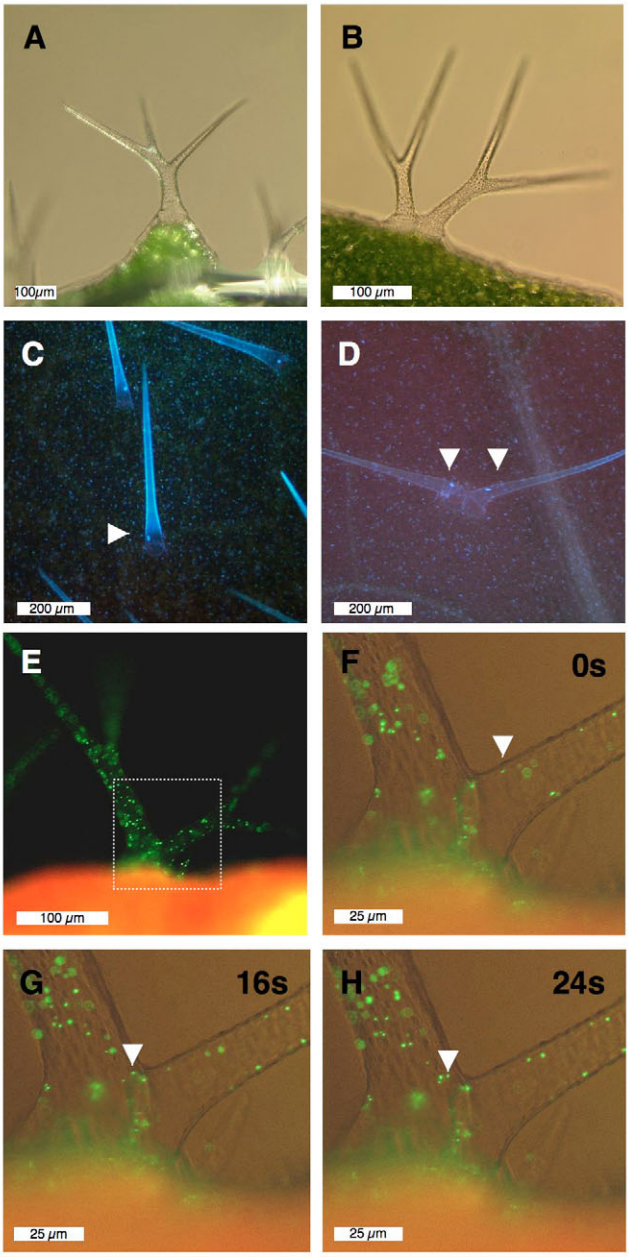

Fig. 1. *elc* mutant trichome phenotype. (**A**) Wild-type trichome. (**B**) *elc* mutant trichome mimicking a trichome cluster. (**C**) DAPI-stained *sti* trichome. Arrowhead marks the polyploid nucleus. (**D**) DAPI-stained *sti elc* double mutant trichome with two stems, each containing a nucleus (arrowheads). (**E-H**) *elc* mutant trichome in which a peroxisome marker is expressed. The boxed area in E is shown in F-H at higher magnification at different time points (s, seconds). The path of a single peroxisome from one trichome to the next is indicated by the arrowhead.

were set to 25 ml running volume (P buffer) at 0.35 ml/minute. The column was equilibrated with three column volumes and calibrated with thyroglobulin (660 kDa), β-amylase (200 kDa), alcohol dehydrogenase (140 kDa) and ovalbumin (43 kDa). Fractions (0.4 ml) were collected, precipitated with trichloroacetic acid and resuspended in protein sample buffer (Laemmli, 1970).

Immunoprecipitation of ESCRT I complex

Protein extracts were made from plants overexpressing the ELC-HA construct under control of the CMV 35S promoter. Plants were grown on hygromycin (25 μg/ml) for 14 days at 22°C under long-day conditions. Plants (0.9 g) were ground in 1.4 ml lysis buffer [50 mM Tris HCl (pH 8.0), 150 mM NaCl, 1% Triton X-100] complemented with 100 μl protease inhibitor (one tablet Complete Protease Inhibitor in 2 ml lysis buffer) and 17.5 μl 1 M DTT. A 1 ml aliquot of this lysate was used with 120 μl anti-HA MicroBeads (Miltenyi Biotec) according to the manufacturer's instructions with the following modifications: the column was rinsed five times with 200 μl Wash Buffer 2, and the protein was eluted with 60 μl Elution Buffer. PAGE was performed using 12% polyacrylamide gels.

Protein identification by peptide mass fingerprinting

After PAGE, the gel was silver-stained as described previously (Blum et al., 1987). Bands were excised and analyzed by MALDI-TOF mass spectrometry (Bioanalytics Centre for Molecular Medicine, Cologne, CMMC).

Protein bands were excised from the gel, treated three times with acetonitrile:water (1:1), once with acetonitrile, reswollen in 50 mM NH_4HCO_3 and dried in a speedvac. Then, 10 mM DTT in 50 mM NH_4HCO_3 was added and the proteins reduced for 45 minutes at 56°C. To alkylate reduced cysteine residues, the remaining liquid was removed and the probe incubated with 50 mM iodoacetamide in 50 mM NH_4HCO_3 for 30 minutes in the dark. Thereafter, the gel pieces were washed and dried as above. The gel pieces were treated for 1 hour with 12.5 ng/μl trypsin (sequencing grade, Promega) in 25 mM NH_4HCO_3, 10% acetonitrile, then washed in the same buffer without enzyme and the proteins digested at 37°C overnight. The digest was stopped by the addition of 5 to 20 μl 1% trifluoroacetic acid (TFA), and the peptides extracted for 30 minutes at 37°C.

A 1.0 μl aliquot of the extracted peptides was mixed with 1.2 μl 2.5 mg/ml 2,5-dihydroxybenzoic acid in 0.1% TFA:acetonitrile (2:1) and spotted onto a 800 μm anchor target (Bruker Daltonics, Bremen, Germany). Positive ion spectra were acquired on a Reflex IV MALDI-TOF mass spectrometer (Bruker Daltonics) in the reflectron mode. A peptide calibration standard (Bruker Daltonics) was used for external calibration of the mass range from m/z 1046 to m/z 3147. Proteins were identified from MALDI fingerprint data by searching the NCBInr public database (release 20060315) using a local installation of MASCOT 1.9.

Cell culture, protoplast isolation and transfection

Arabidopsis cell suspension culture (Columbia ecotype; grown in MS medium supplemented with 0.5 mg/l NAA and 0.1 mg/l KIN) was maintained as described (Mathur and Koncz, 1998). Protoplast isolation and polyethylene glycol-mediated transfection were performed according to Magyar and co-workers (Magyar et al., 2005). The transfected cells were incubated at 23°C for 16 hours in the dark before staining and microscopic observation.

For YFP and FM4-64 double-labeling and co-transfection, YFP-ELC was introduced into the protoplasts of *Arabidopsis* suspension culture cells as described above. After 16 hours incubation in MS cell culture medium containing 0.34 M glucose, 0.34 M mannitol, protoplasts were collected by centrifugation, resuspended in the same medium containing 50 μM FM4-64, and placed on ice for 10 minutes (Ueda et al., 2001). After labeling, cells were washed twice, resuspended in the same medium without FM4-64 and analyzed.

Microscopy and cell biology

The C value of trichome nuclei was determined using the DISCUS software package (Carl H. Hilgers-Technisches Büro, Königswinter, Germany). The fluorescence intensity of DAPI-stained nuclei was determined, and the relative fluorescence units (RFU) were calibrated with stomata trichome nuclei that have a DNA content of 2C (Galbraith et al., 1991). Light microscopy was performed with a Leica DMRE microscope (Leica, Wetzlar, Germany) equipped with a high-resolution KY-F70-3CCD JVC camera and frame-grabbing DISKUS software. Confocal microscopy was performed using a TCS SP2 (Leica). Leaf sections were stained with 500 μg/ml propidium iodide and infiltrated for 15 minutes at 0.9 bar. After staining, leaves were embedded in 5% low-melting-point agarose and sectioned with a razor blade. Images were processed using Adobe Photoshop 6.0 software.

Yeast transformation and yeast two-hybrid assay

The yeast strain AH109 (Halladay and Craig, 1996) was grown in standard yeast full media or selective drop-out media (Clontech) under standard conditions.

Transformation of plasmids into yeast was performed using the Lithium acetate method (Gietz et al., 1995). Interactions were analyzed on synthetic drop-out medium lacking leucine and tryptophan and on synthetic drop-out medium without leucine, tryptophan and histidine supplemented with 3 mM 3-aminotriazole (3-AT) (Sigma-Aldrich, Munich, Germany) after 3 days of growth. SNF1 and SNF4 were used as positive controls (Fields and Song, 1989). The interaction between ELC and VPS37-1 was observed in eight independent experiments.

RESULTS

The *elc* mutant affects trichome morphogenesis

The *elc* mutant was initially discovered in a T-DNA collection from Versailles because of a subtle trichome cluster phenotype. Wild-type trichomes are single polyploid cells with three to four branches (Fig. 1A). In *elc* mutants, about 2% of the trichomes showed a cluster phenotype (n=3529). In clusters, two stems were usually formed that appeared to separate just above the epidermal surface giving the trichome a moose-horn-like appearance (Fig. 1B). Each of the stems

Table 1. Cluster frequencies and multinucleated trichome cells in *elc* crosses and control lines

Genotype	Cluster frequency (%)*	Stems/cluster	Branch points	Nuclei/cluster	n
Ws2	0	/	1.62±0.50	/	2971
Ler	0	/	1.99±0.21	/	2253
elc (Ws2)	1.93	2.03±0.17	1.04±0.69†	1.97±0.34	3529
elc (Ler)‡	1.66	2.13±0.34	1.92±0.29†	1.87±0.52	963
stichel146	0	/	0±0	/	463
kaktus (Ler)	0	/	3.32±0.60	/	1106
kaktus (Ws)§	0	/	3.23±0.66	/	1373
tfc-a (Ws2)	0.81	2.09±0.30	0±0	2.27±0.65	1356
stichel146 elc	1.07	2±0	0.04±0.30†	1.85±0.60	2060
kaktus elc	1.74	2.08±0.27	1.85±0.98†	1.94±0.59	2924
tfc-a elc	16.29	2.13±0.43	0.32±0.52†	2.43±0.59	743

*In the context of this paper, clusters are defined as trichomes with two stems emerging from one single trichome cell.
†Branch point number for each stem of a clustered trichome.
‡More than 20 plants of an F2 cross between *elc* and wild type ecotype L*er* showing *elc* mutant phenotype were analysed.
§More than 20 plants of an F2 cross between *kak* and wild type Ws2 showing *kak* mutant phenotype were analysed.

was slightly less branched than wild type (Table 1). To test whether the unusual morphology of *elc* mutants was due to an aberrant branch initiation, we generated a double mutant with the *stichel* (*sti*) mutant. Mutations in *STI* resulted in unbranched trichomes (Fig. 1C). The *elc sti* double mutant showed cluster-like trichomes lacking additional branches (Fig. 1D; Table 1). This suggests that the induction of two trichomes is unrelated to branching. In order to determine whether the clusters represent two separate trichomes or a single cell producing two stems, we introduced a construct into the *elc* mutant line that specifically labels peroxisomes, which move along the actin cytoskeleton (Mathur et al., 2002). When tracing the path of single peroxisomes we found them moving from one stem into the other, demonstrating that the two stems belong to one cell (Fig. 1E-H).

elc mutants exhibit several nuclei in various cell types

A closer phenotypic analysis revealed that about 2% of all trichomes had more than one nucleus (Table 2). Among the cluster-like trichomes, 93% had several nuclei (Fig. 2B-F), whereas 0.4% of the trichomes with a normal appearance had more than one nucleus (Fig. 2G). This suggests that the formation of additional trichome stems could be induced by the presence of additional nuclei. During wild-type development, trichome cells proceed through four endoreduplication cycles resulting in a final DNA content of 32C (Hulskamp et al., 1994). If *ELC* acts at the switch from mitosis to endoreduplication, either of two scenarios could occur in *elc* mutants. First, an incomplete cell division could take place instead of the first endoreduplication cycle. In this case, the total DNA content of each

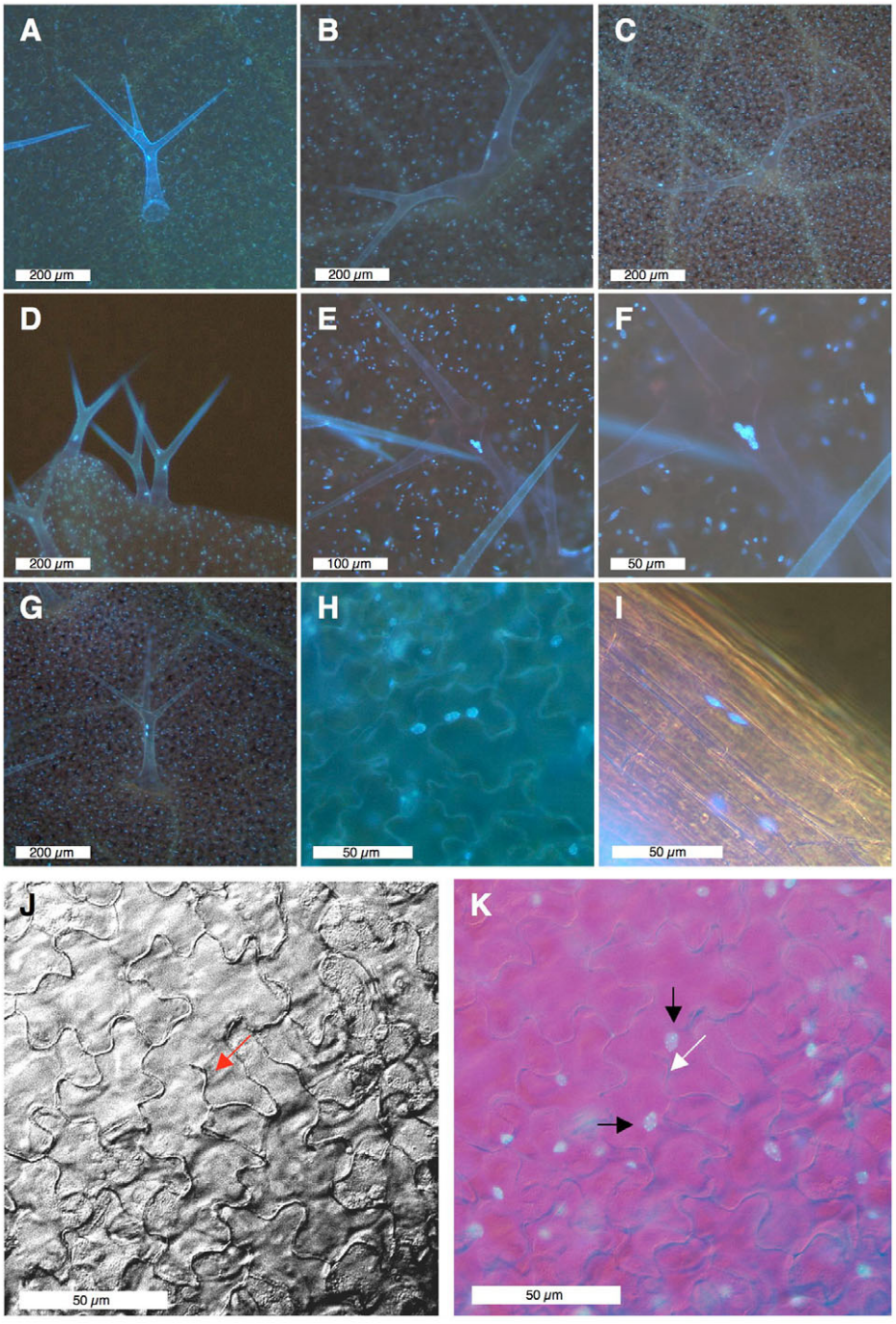

Fig. 2. Cytokinesis defects in *elc* mutants. The nuclear phenotypes of wild type and *elc* were shown by DAPI staining. (**A**) Wild-type trichome with one nucleus located at the branch point. (**B-F**) *elc* mutant trichomes with two nuclei in one stem (B), one nucleus in each stem (C), with three nuclei (D) and with four nuclei (E). (F) Higher magnification of E. (**G**) Occasionally, trichomes with a wild-type appearance have two nuclei. (**H**) Multiple nuclei in epidermal pavement cells. (**I**) Multiple nuclei in hypocotyl cells. (**J**) Incomplete cell wall in an epidermal pavement cell (red arrow). (**K**) DAPI staining of J to indicate the position of the two nuclei in the cell (black arrows); the white arrow marks the incomplete cell wall.

Table 2. Frequency of multinucleate cells in different cell types in *elc* mutants

	Trichomes	Epidermal cells	Hypocotyl cells	Stomata
Frequency of multinucleated cells in *Ws2* (%)	0	0.221	0.096	0
n	2971	1807	2088	1745
Frequency of multinucleated cells in *elc* (%)	2.30	0.67*	2.1*	0
n	3529	3448	2339	1843

*The mutant shows significantly higher frequencies than wild type (95%, Odd Ratio test).

of the two nuclei should be 16C and the total cellular DNA content should be 32C. Second, the first incomplete cell division might be followed by the normal trichome differentiation program; in this case, each of the two nuclei would be 32C and the total DNA content would be doubled. When measuring the DNA content of nuclei in *elc* mutants, we found that individual nuclei in *elc* trichomes containing one or two nuclei had a DNA content of approximately 32C (Fig. 3), suggesting that the second scenario is true.

The multiple nuclei phenotype is not specific to trichomes but was also found in other cells. Epidermal pavement cells and hypocotyl cells showed multiple nuclei (Fig. 2H,I), though the frequency was generally lower than in trichomes (Table 2). We occasionally observed epidermal cells with incomplete cell walls, further supporting the contention that *ELC* is involved in the regulation of cell divisions (Fig. 2J,K). However, out of 1843 stomata cells, not a single cell with multiple nuclei was found (Table 2).

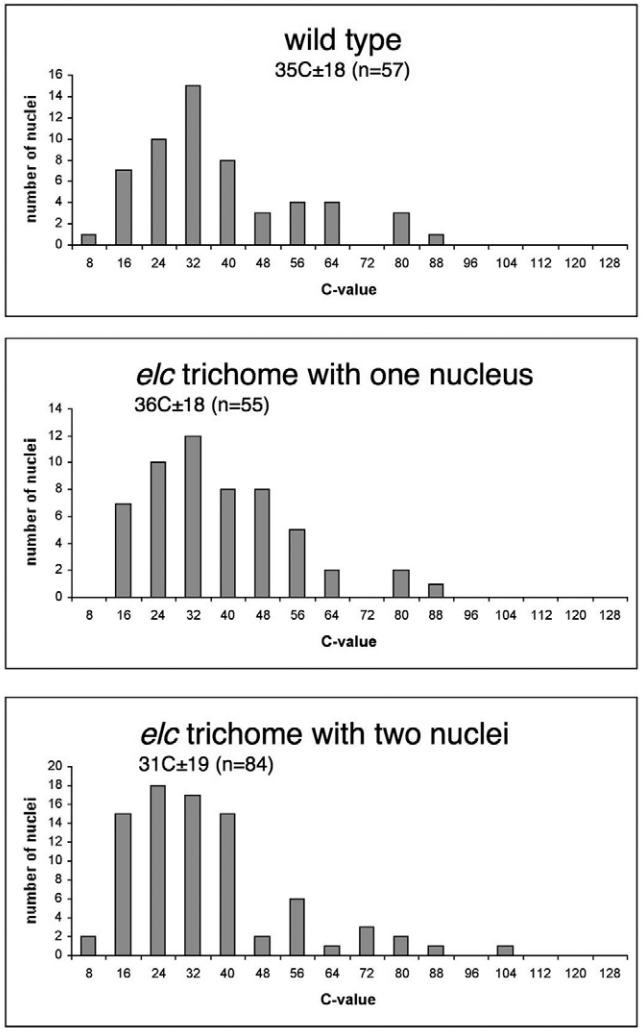

Fig. 3. DNA content of nuclei in *elc* mutants. Comparison of the DNA content of trichome nuclei of wild-type (top) and *elc* mutant trichomes containing one (middle) or two nuclei (bottom). The relative distribution and the average nuclear DNA content of individual nuclei are very similar in all three situations.

The *ELC* gene encodes the *Arabidopsis* Vps23/TSG101 homolog

The flanking sequences of the left border revealed a T-DNA insertion between the two genes At3g12390 and At3g12400. The left border was located 43 bp downstream of At3g12390; the genomic sequences flanking the right border could not be amplified. A genomic fragment of At3g12390 did not rescue the *elc* mutant phenotype, whereas a 2.9 kb genomic fragment of the At3g12400 gene covering the region between the two neighboring genes showed full rescue of the *elc* mutant phenotype. This fragment contains 600 bp of the 5′ region and 1.1 kb of the 3′ region (Fig. 4A). Also, overexpression of the At3g12400 gene under the CaMV 35S promoter rescued the *elc* mutant. No additional phenotypes were observed in the *ELC* overexpression lines. To determine the T-DNA insertion site, we performed TAIL-PCR with primers located close to the 5′ end of the *ELC* gene. The T-DNA was inserted 786 bp after the start codon of *ELC* (Fig. 4B). The inserted sequence leads to a stop codon after a further 30 bp, and a predicted protein lacking the C-terminal 166 amino acids (Fig. 4C). RT-PCR experiments revealed that the expression of mutant *ELC* RNA was strongly reduced (Fig. 5B). To exclude the possibility that low levels of truncated ELC protein have a dominant negative effect, we expressed the truncated version of ELC under the 35S promoter in the wild type. Out of 150 transformants, not a single line showed an *elc*-like phenotype.

The *ELC* gene has no introns and shows sequence similarity to the yeast Vps23 and mammalian *TSG101* genes (60% positives and 11% identical, amino acid level) (Fig. 4D). Although the overall similarity is not high, the three genes do share a similar size and arrangement of domains (Fig. 4E). At the N-terminus, all three share a ubiquitin conjugating enzyme variant (UEV) domain that is missing a cysteine conserved in ubiquitin conjugating (UBC) domains. According to the COILS program (Lupas et al., 1991), a coiled-coil region is located in the middle part of the protein. At the C-terminus is located a conserved domain termed the steadiness box because it is involved in the control of the stability of TSG101 (Feng et al., 2000). The *Arabidopsis* genome contains, in addition to *ELC*, a close homolog (72% identity) with the same domain structure and without the crucial cysteine in the UEV domain. *ELC* homologs are also present in monocotyledons such as rice (Fig. 4D).

The expression of *ELC* was determined by RT-PCR. Expression was found in all tissues analyzed including roots, stems, leaves and flowers (Fig. 5A). These results are consistent with the expression data published in GENEVESTIGATOR (www.genevestigator.ethz.ch).

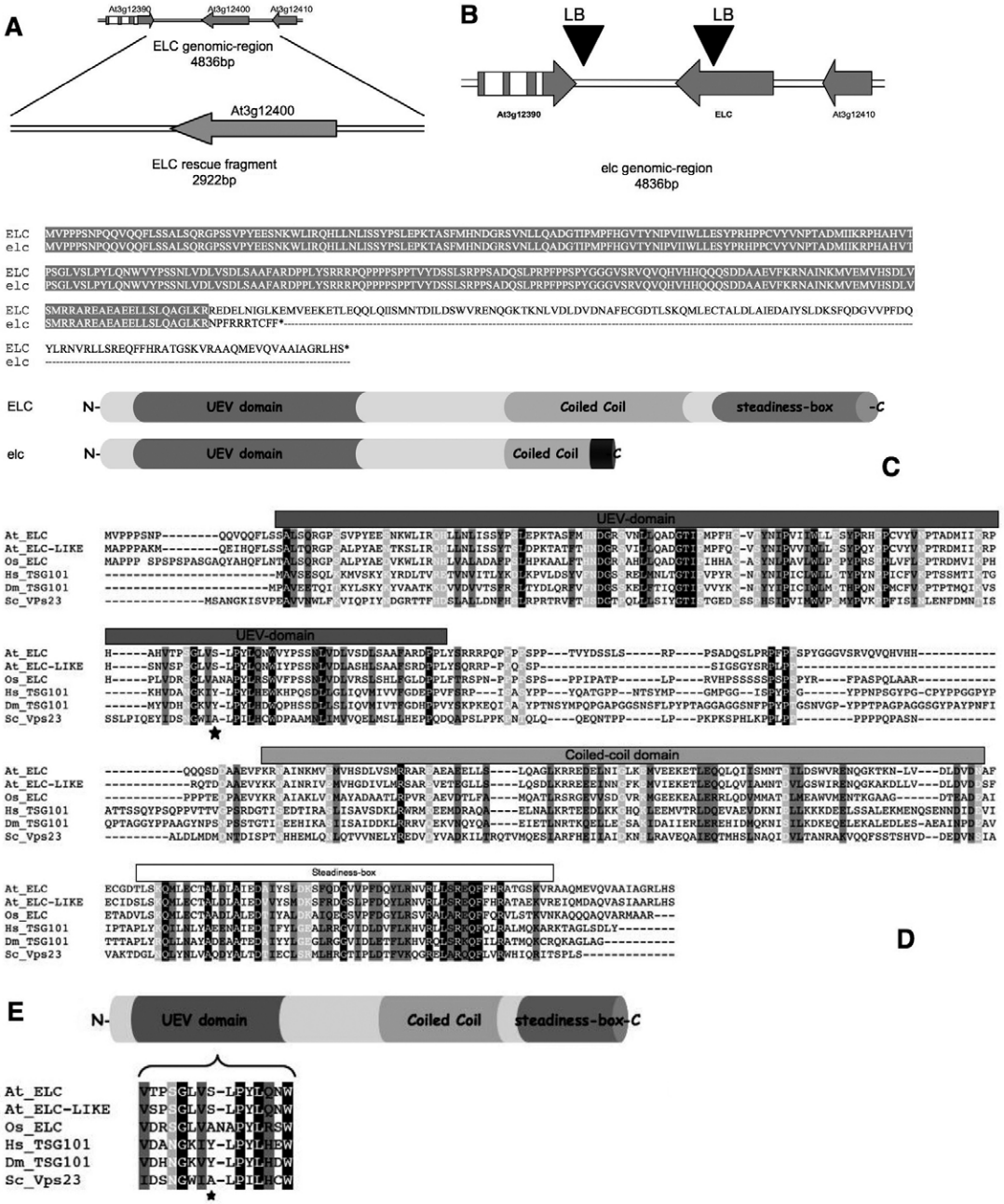

Fig. 4. Molecular analysis of the *ELC* gene. (**A**) Schematic of the chromosomal region of the *ELC* gene. The fragment used for the rescue experiments is indicated. (**B**) The chromosomal region of the *ELC* gene shows two insertions in the mutant. (**C**) The insertion in the *ELC* gene results in a truncated protein. A sequence alignment of the wild-type and mutant proteins and a schematic highlighting their domain structure are shown. (**D**) Sequence alignment of ELC (At3g12400) and ELC-like (At5g13860) from *Arabidopsis thaliana* (At), ELC from *Oriza sativum* (Os) (BAD28453), yeast Vps23 (Sc) (Af004731), human TSG101 (Hs) (U82130) and *Drosophila* TSG101 (Dm) (NM_079396). Letters in a black background indicate identity, dark gray backgrounds indicate strong similarity and a light gray background indicates weak similarity. (**E**) Schematic of the protein domain arrangement of ELC, TSG101 and Vps23. The characteristic absence of a cysteine conserved in UBC domains (star) is depicted below.

The genes of the ESCRT I-III pathway are conserved in plants

In yeast, Vps23p is part of a mono-ubiquitylation-dependent protein sorting pathway in which Vps23p binds ubiquitin through its UEV domain, which shows sequence similarity to E2 conjugating enzymes (Katzmann et al., 2001). Vps23p is part of the ESCRT I complex which consists of three subunits, Vps23p, Vps28p and Vps37p, which belong to the class E vacuolar sorting proteins (Bankaitis et al., 1986; Banta et al., 1988; Odorizzi et al., 1998; Raymond et al., 1992). Subsequently, further downstream class E Vps proteins are activated that form the ESCRT II and ESCRT III complex that mediate the actual protein sorting (Babst et al., 2002a; Babst et al., 2002b; Katzmann et al., 2001). A detailed database search revealed that homologs of all components of the ESCRT I, II and III complexes are present in the *Arabidopsis* genome (Table 3).

ELC binds ubiquitin in vitro

The presence of a UEV domain suggests that ELC can bind to ubiquitin. To test this, an HA tag was fused to the C-terminus of ELC and expressed in *Escherichia coli* under control of the T7 promoter, and in *elc* mutant plants under the control of the 35S promoter. Expression was measured by semi-quantitative RT-PCR and compared with wild-type and *elc* plants. The ELC-HA fusion construct rescued the *elc* mutant phenotype indicating functionality of the fusion protein. On western blots, the plant-expressed ELC-HA was slightly larger than the expected 43 kDa and migrated at 49 kDa. Protein was extracted from transgenic plants and used in a pull-down assay with ubiquitin-agarose. ELC-HA was precipitated with ubiquitin-agarose but not with the control Protein-G–agarose (Fig. 6), suggesting that ELC can bind ubiquitin.

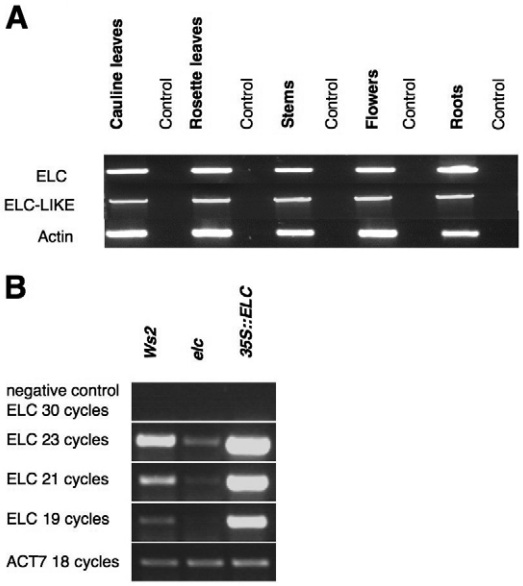

Fig. 5. Expression analysis of *ELC*. (**A**) Expression of *ELC* and *ELC*-like in different tissues. As control for genomic contamination, the different RNAs were used as templates without reverse transcriptase. (**B**) Semi-quantitative RT-PCR to compare the RNA levels of wild type (Ws2), *elc* mutant and a 35S:*ELC* overexpression line.

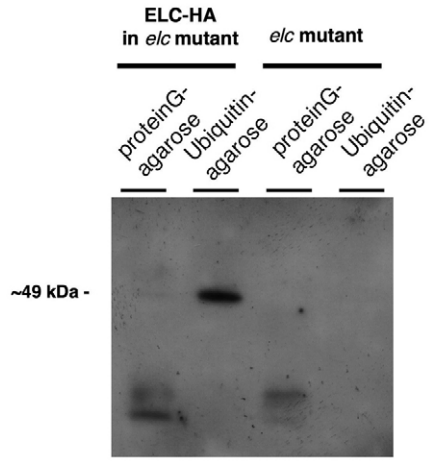

Fig. 6. Ubiquitin binding of ELC. Pull-down assays were performed using ubiquitin coupled to agarose and the ELC-HA protein was detected on the western blot using an anti-HA antibody. Protein G coupled to agarose was used as a control.

ELC is a component of a high-molecular-weight protein complex

The yeast homolog of ELC, Vps23p, has been found in a large complex of about 350 kDa (Babst et al., 2000). In order to test whether the plant homolog is also part of a complex, we used the ELC-HA transgenic lines described above. Upon separation on a Superose 6 10/300 GL gel filtration column, we detected ELC-HA in a size range between 200 and 400 kDa (Fig. 7).

ELC interacts with components of the ESCRT I complex

In order to identify proteins interacting with ELC we performed co-immunoprecipitation and subsequent protein identification by peptide mass fingerprinting in MALDI-TOF mass spectrometry using ELC-HA transgenic plants. We were able to identify proteins from three gel bands (Fig. 8). One band corresponded to ELC-HA. The second band, of approximately 26 kDa, yielded fragments of the VPS37-1 protein. The third band, of approximately 24 kDa, contained the *Arabidopsis* VPS28-1 homolog.

These data are consistent with studies in mammals where VPS37 is known to interact with TSG101 (Bache et al., 2004; Eastman et al., 2005; Stuchell et al., 2004). The interaction between VPS37-1

Table 3. Comparison of ESCRT I-III like proteins between yeast, mammals and *Arabidopsis*

Saccharomyces	Ident./simil. to *Arabidopsis* (%)	Mammals	Ident./simil. to *Arabidopsis* (%)	*Arabidopsis*	*Arabidopsis* locus name
ESCRT I		**ESCRT I**		**ESCRT I**	
Vps23p/Stp22	19/33	TSG101	25/39	ELC	At3g12400
	19/34		24/37	ELC-like	At5g13860
Vps28p	32/47	VPS28	35/51	VPS28-1	At4g21560
	31/46		35/52	VPS28-2	At4g05000
Vps37p	18/29	VPS37	9/16	VPS37-1	At3g53120
	18/29		9/16	VPS37-2	At2g36680
ESCRT II		**ESCRT II**		**ESCRT II**	
Vps22p	24/34	EAP30	35/43	VPS22	At4g27040
	9/15		14/19	VPS22	At3g31960
Vps25p	25/40	EAP25	33/48	VPS25	At4g19003
Vps36p	13/24	EAP45	6/13	VPS36	At5g04920
ESCRT III		**ESCRT III**		**ESCRT III**	
	26/38		55/74	VPS2	At2g06530
Vps2p	18/31	CHMP2	34/56	VPS2	At1g03950
	19/32		35/55	VPS2	At5g44560
Vps20p	28/41	CHMP6	33/49	VPS20	At5g63880
	29/41		33/50	VPS20	At5g09260
Vps24p	30/50	CHMP3	39/57	VPS24	At5g22950
	22/40		33/47	VPS24	At3g45000
Vps32p	29/40	CHMP4	33/44	VPS32	At2g19830
	30/44		36/47	VPS32	At4g29160

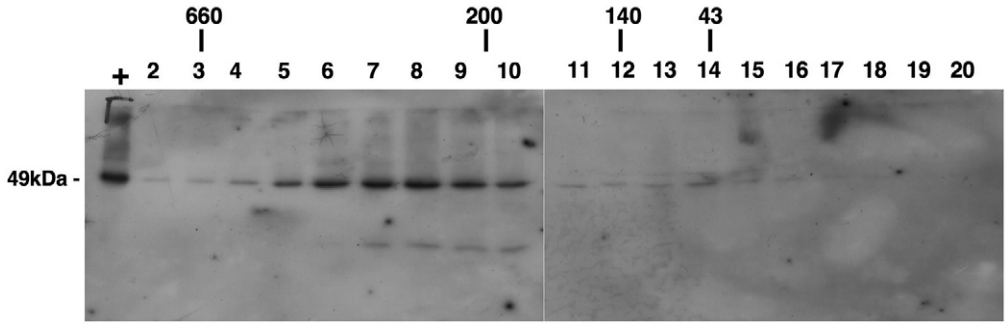

Fig. 7. ELC is a component of a large protein complex. Protein extract was loaded on a Superose 6 10/300 GL gel filtration column, separated on an SDS-PAGE gel and ELC-HA detected by western blotting. The following size markers were used: thyroglobulin (660 kDa), β-amylase (200 kDa), alcohol dehydrogenase (140 kDa) and ovalbumin (43 kDa).

and ELC was additionally confirmed by a yeast two-hybrid assay using both genes as bait and as prey. As summarized in Table 4, interactions were found between the two proteins. In summary, these data show that ELC is part of the plant ESCRT I complex.

YFP:ELC is localized to endosomal compartments

To study the intracellular localization of ELC in living cells, we fused yellow fluorescent protein (YFP) and cyanin fluorescent protein (CFP) to the N-terminus of ELC. We confirmed the functionality of the YFP-ELC fusion protein by rescuing *elc* mutant plants with a 35S:YFP-ELC construct. YFP-ELC was transiently expressed in *Arabidopsis* protoplasts derived from cell suspension cultures, and the cells stained with FM4-64. The lipophilic styryl dye FM4-64 is a marker for endocytic intermediates and enables the visualization of transport processes from the plasma membrane via endosomes to the vacuole in vivo (Vida and Emr, 1995). As shown in Fig. 9, the small compartments showing YFP-ELC staining were also stained with FM4-64. This demonstrates that ELC is localized to the endosomes. We also found FM4-64-labeled compartments without YFP fluorescence, indicating that ELC is not present in all endosomal compartments (Fig. 9A-D). To determine more specifically the stages at which ELC is localized to the endosome, we co-transfected CFP-ELC with Ara6-GFP, as a marker for early endosomes, or with GFP-Ara7, as a marker for late endosomes (Ueda et al., 2001). We found co-localization of CFP-ELC with both Ara6-GFP (Fig. 9E-H) and GFP-Ara7 (Fig. 9I-L), indicating that ELC is localized to early and late endosomes.

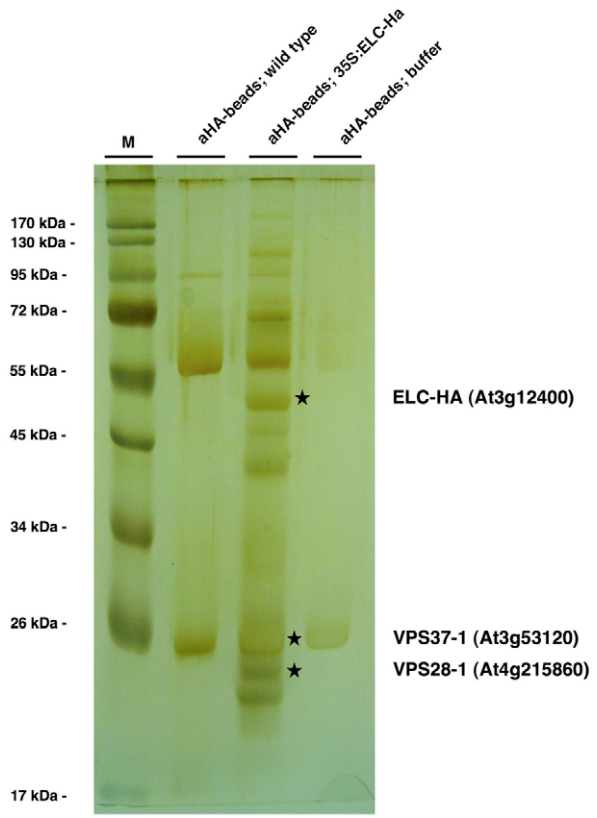

Fig. 8. Co-immunoprecipitation of ESCRT-I proteins with ELC-HA. Using anti-HA beads, ELC-HA was immunoprecipitated from protein extracts and separated by PAGE. MALDI-TOF analysis revealed indicative fragments for the three bands marked by a star: ELC-HA, VPS37-1 and VPS28-1.

Genetic independence of the ELC pathway and the putative E3 ligase KAKTUS proteasome pathway

The *kaktus* (*kak*) mutant has an increased ploidy level of 64C, indicating that the number of endoreduplication cycles is limited by *KAK*. It has been proposed that KAK is involved in protein degradation because it encodes a putative ubiquitin E3 ligase (Downes et al., 2003; El Refy et al., 2004). The *kak elc* double mutant exhibited an additive trichome phenotype. The cluster frequency and number of nuclei was similar to that in *elc* mutants (Table 1) and the number of branches was similar to that in *kak* mutants. Thus, additional endoreduplication cycles do not lead to more nuclei in the *elc* mutant background, suggesting that the *ELC* gene is not important during endoreduplication cycles but at the initial switch from mitosis to endoreduplication. The additive phenotype provides no hint towards a redundant function of the ELC-dependent pathway and the putative E3 ligase KAKTUS-dependent proteasome pathway.

Genetic evidence suggests that *ELC* controls nuclear divisions through the microtubule cytoskeleton

Several pathways are known by which the ESCRT I-III pathway controls the cell cycle in animals. However, the absence of the relevant components of these pathways renders it unlikely that these pathways are operating in plants (for details see Discussion). Because several examples are known in which microtubule misregulation results in multinuclear cells in plants (Kirik et al.,

Table 4. Interaction of ELC with Vps37 in the yeast two-hybrid system

Bait (pAS)	Prey (pACT)	Interaction
ELC	Vps37 (At2g36680)	+
Vps37 (At2g36680)	ELC	+
ELC	pACT	–
Vps37 (At2g36680)	pACT	–
SNF1	SNF4	+

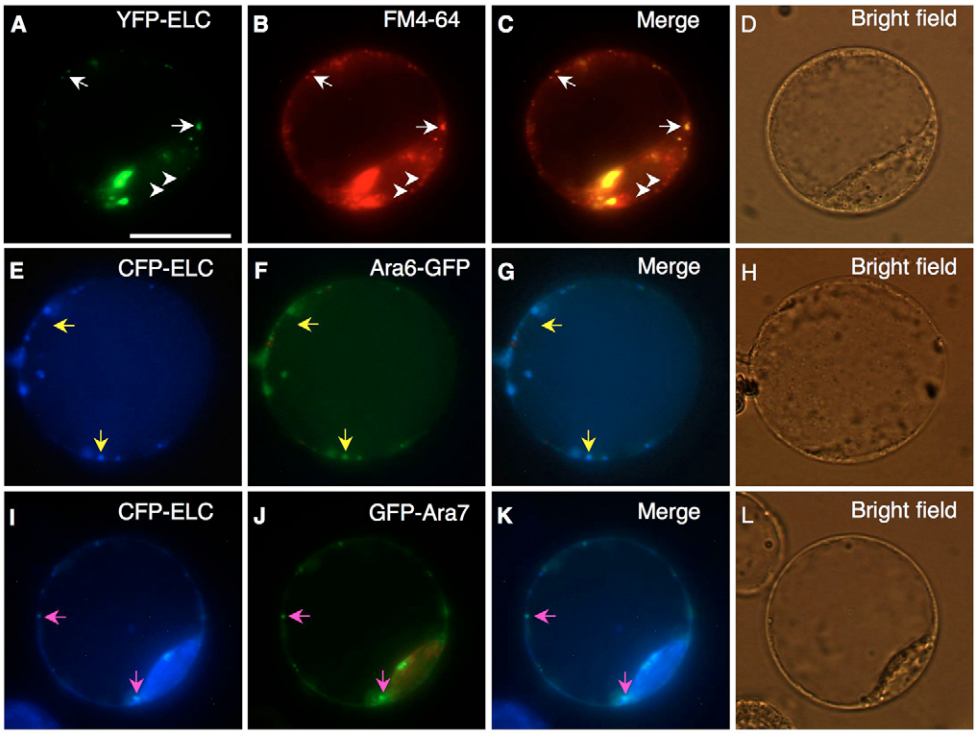

Fig. 9. ELC localizes to endosomes. (**A-D**) Protoplasts of *Arabidopsis* cultured cells expressing YFP-ELC (A) were labeled with FM4-64 (B). The small dots with YFP-ELC (white arrows) were also stained by FM4-64. Note that few dots labeled by FM4-64 were not marked by YFP-ELC (arrow heads). (**E-L**) CFP-ELC (E,I) was co-transfected with Ara6-GFP (F) and with GFP-Ara7 (J) into protoplasts of *Arabidopsis* cultured cells. The dots with CFP-ELC co-localized with Ara6-GFP (yellow arrows) and also with GFP-Ara7 (pink arrows). Scale bar: 20 μm.

2002a; Kirik et al., 2002b; Muller et al., 2004; Steinborn et al., 2002), we speculated that ELC controls nuclear divisions through the microtubule cytoskeleton. To test this hypothesis, we created an *elc kiesel-T1 (kis-T1)* double mutant. The *KIS* gene encodes a homolog of tubulin-folding cofactor A, a component of a pathway important for the formation of assembly competent α/β tubulin dimers (Kirik et al., 2002a; Steinborn et al., 2002). Strong *KIS* mutants have multiple nuclei and are embryo lethal (Steinborn et al., 2002). We used the weak *kis-T1* mutant that displays a mild growth defect, slightly reduced cell division frequency, reduced trichome branching and occasionally cells with multiple nuclei (Kirik et al., 2002a). The double mutant showed a synergistic phenotype: the frequency of trichomes with more stems was drastically increased (16%; *n*=743) as compared with *elc* (2%; *n*=3529) and *kis-T1* (0.8%; *n*=1356) (Fig. 10A-F). Epidermal pavement cells were strongly reduced in size (Fig. 10G-I), the leaf architecture was grossly disturbed (Fig. 10J-L) and many cells contained multiple nuclei and nuclear anomalies (Fig. 10M-O). The strong mutual enhancement of the phenotypes indicates that the two genes act in the same pathway and hence that ELC regulates cell division at least in part through the microtubule cytoskeleton.

DISCUSSION

It is well established that poly-ubiquitylation of proteins and their degradation by the 26S proteasome plays a crucial role in the regulation of the cell cycle. A new emerging pathway is the regulation of the cell cycle by mono-ubiquitylation-mediated protein degradation (Babst et al., 2000; Urbanowski and Piper, 2001). In this pathway, mono-ubiquitylated proteins are targeted to the late endosome, the so-called MVB. After fusion of the MVB with the vacuole (in yeast) or the lysosome (in animals), proteins become accessible to proteases and are degraded. A regulation of the cell cycle by this pathway is suggested by the finding that mutations in human TSG101, which is involved in sorting mono-ubiquitylated proteins into the MVB (Katzmann et al., 2001), lead to mitotic defects including multiple MTOCs (microtubule organizing centres), misdistribution of chromosomes and multiple nuclei (Xie et al., 1998). Our finding that mutations in the *Arabidopsis* homolog of TSG101 lead to multiple nuclei suggest that a related pathway is operating in plants.

Non-proteasomal protein degradation in lytic vacuoles in plants

Although the Vps23p/TSG101 pathway has not been described in plants, it has been shown that lytic vacuoles similar to those in yeast exist (Swanson et al., 1998). Plant cells can have two different types of vacuoles (Paris et al., 1996), a lytic and a protein storage vacuole (Swanson et al., 1998; Vitale and Raikhel, 1999). These two different vacuoles seem to fuse in mature cells to form the central vacuole. Newly synthesized proteins enter different routes for the lytic and the storage vacuoles (Bassham and Raikhel, 2000). Proteins destined for the storage vacuole are found in PACs (precursor accumulating vesicles) before they reach the vacuole. Alternatively, proteins may be routed via DVs (dense vesicles) and the MVB (Tse et al., 2004). Proteins targeted to the lytic vacuole are found in the CCV (clathrin-coated vesicles) and the PVC (prevacuolar compartment) before they reach the lytic vacuole.

The ESCRT-pathway in plants

To date, there is no biochemical evidence for the existence of a mono-ubiquitin-dependent protein-sorting pathway in plants. At present, this excludes the possibility to directly test a function of ELC in protein sorting. However, the overall sequence similarity and the conserved arrangement of domains suggest that *ELC* encodes a Vps23p/TSG101 homolog. That *ELC* acts in a Vps23p/TSG101 pathway is indicated by four observations. First, the complete ESCRT machinery known from yeast is conserved in *Arabidopsis*. All three subunits of the ESCRT I complex, Vps23p, Vps28p and Vps37p, were found. The three subunits comprising the ESCRT II complex, Vps22p, Vps25p and Vps36p, and those of the ESCRT III

complex, Vps2p, Vps20p, Vps24p and Snf7, are all present in the *Arabidopsis* genome (see also Winter and Hauser, 2006). Second, we found that the ELC protein binds ubiquitin in vitro. Third, ELC is part of a high molecular weight complex and binds directly to VPS37 and VPS28, two components of the ESCRT I complex, as has been shown for the mammalian TSG101 (Bache et al., 2004; Eastman et al., 2005; Stuchell et al., 2004) and for Vps23p in yeast (Katzmann et al., 2001). Forth, YFP:ELC co-localizes with the endocytotic markers FM4-64 (Vida and Emr, 1995), ARA6 and ARA7 (Ueda et al., 2001), indicating that ELC localizes to early and late endosomes.

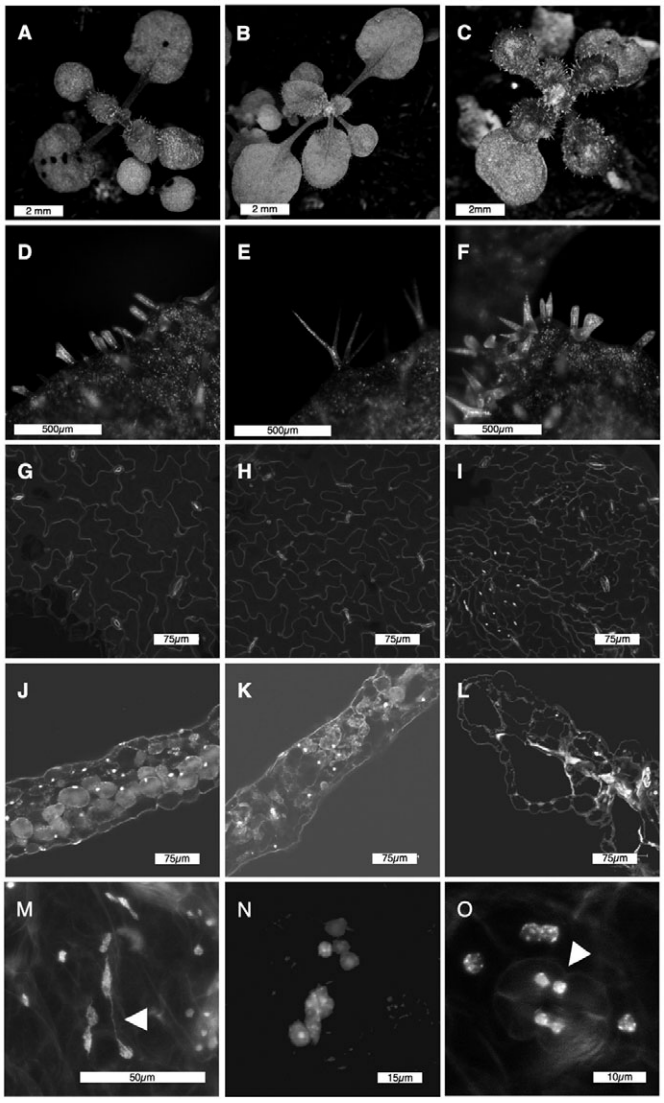

Fig. 10. Analysis of the *elc kis-T1* double mutant.
(**A-C**) Comparison of *kis-T1* (A), *elc* (B) and *kis-T1 elc* (C) mutant rosette leaves. (**D-F**) Comparison of *kis-T1* (D), *elc* (E) and *kis-T1 elc* (F) mutant trichomes. Note that the cluster frequency is strongly enhanced in the double mutant. (**G-I**) Comparison of *kis-T1* (G), *elc* (H) and *kis-T1 elc* (I) mutant epidermal pavement cells. Cell size is reduced in the double mutant. (**J-L**) Comparison of *kis-T1* (J), *elc* (K) and *kis-T1 elc* (L) sections of rosette leaves. The integrity of the leaf is strongly disturbed in the double mutant. (**M-O**) Higher magnification of propidium iodide-stained leaf sections from *kis-T1 elc* double mutants. Multinucleated cells are frequently observed in the *kis-T1 elc* double mutants. Nuclear anomalies like nuclear bridges (arrowhead, M) and high numbers of nuclei per cell (N) were found frequently. In very rare cases, multinucleated stomata with incomplete cell walls were observed (arrowhead, O).

The role of the Vps23p/ELC/TSG101-pathway in cell divisions

The multinuclear phenotype found in *elc* mutants indicates that ELC is involved in the regulation of cell division. The finding that *ELC* encodes a component of a putative mono-ubiquitin-dependent protein degradation pathway raises the question of which cell division factors are targeted. In animals, a role for TSG101 in cell division is evident from the finding that mutations in human TSG101 lead to cell division defects including multiple MTOCs, misdistribution of chromosomes and multiple nuclei (Xie et al., 1998). The molecular link to the cell cycle is still unclear and three possibilities that are not mutually exclusive are currently discussed: (1) Because it has been shown that cell-cycle relevant receptors (e.g. the EGF-receptor) are subject to TSG101-dependent degradation, it is assumed that the cell division phenotype is caused by a failure to degrade these receptors (Babst et al., 2000; Carter and Sorkin, 1998); (2) A second possibility is that TSG101 is involved in the control of the known cell cycle regulator p53. It has been shown that TSG101 is part of a regulatory circuitry with MDM2 and p53 (Haupt et al., 1997; Kubbutat et al., 1997; Li et al., 2001); (3) A third possibility is that TSG101 controls the stability of $p21^{Cip1}$ (CDKN1A – Human Gene Nomenclature Database), which is a well-characterized inhibitor of CDK activity. It has been shown that TSG101 interacts with $p21^{Cip1}$ in the yeast two-hybrid assay (Oh et al., 2002) and that the stability of $p21^{Cip1}$ was drastically increased in the presence of TSG101.

It is unlikely that these pathways are operating in plants. A true p53 or EGF ortholog has not yet been found in the fully sequenced *Arabidopsis* genome. Also, a clear $p21^{Cip1}$ ortholog is missing. Instead, a class of ICK/KRP proteins sharing a short motif responsible for CDK and cyclin binding exists (Verkest et al., 2005). It is therefore likely that cell division regulation by Vps23p/ELC/TSG101 is mediated by an as yet undescribed route in this context. Our genetic data provide a first hint. The *elc* phenotype is reminiscent of mutants defective in regulators of the microtubule cytoskeleton (Kirik et al., 2002a; Kirik et al., 2002b; Muller et al., 2002; Muller et al., 2004; Steinborn et al., 2002; Twell et al., 2002) and is enhanced in the *elc kis-T1* double mutant. This suggests that the regulation of the microtubule cytoskeleton by *ELC* might be relevant for the regulation of cell division in plants.

Perspectives

Although the phenotype of the first plant mutant in the ESCRT I-III pathway indicates that this pathway is important for the regulation of cytokinesis, it is likely that this occurs through different routes than in animals. It will be imperative to study the ESCRT I-III pathway in plants in more detail. Markers are required to trace the fate of proteins in this pathway. The key challenge will be the identification of proteins that are regulated by this pathway.

We thank members of the laboratory for critically reading the manuscript. We are indebted to Hilmar Ilgenfritz who identified the *elc* mutant. We thank V. Kirik for initiating our work on the connection between *ELC* and microtubule function; Norman Zielke, University of Cologne, for help with the ubiquitin binding assays; Takashi Ueda, University of Tokyo, for providing Ara6-GFP and GFP-Ara7; and the RIKEN Genomic Sciences Centre for providing cDNA for Vps37. This work was supported by grants from the SFB 635 and the Volkswagenstiftung to M.H. C.K. is supported by the NRW International Graduate School for Genetics and Functional Genomics.

References

Babst, M. (2005). A protein's final ESCRT. *Traffic* **6**, 2-9.

Babst, M., Odorizzi, G., Estepa, E. J. and Emr, S. D. (2000). Mammalian tumor susceptibility gene 101 (TSG101) and the yeast homologue, Vps23p, both function in late endosomal trafficking. *Traffic* **1**, 248-258.

Babst, M., Katzmann, D. J., Estepa-Sabal, E. J., Meerloo, T. and Emr, S. D. (2002a). Escrt-III: an endosome-associated heterooligomeric protein complex required for mvb sorting. *Dev. Cell* **3**, 271-282.

Babst, M., Katzmann, D. J., Snyder, W. B., Wendland, B. and Emr, S. D. (2002b). Endosome-associated complex, ESCRT-II, recruits transport machinery for protein sorting at the multivesicular body. *Dev. Cell* **3**, 283-289.

Bache, K. G., Slagsvold, T., Cabezas, A., Rosendal, K. R., Raiborg, C. and Stenmark, H. (2004). The growth-regulatory protein HCRP1/hVps37A is a subunit of mammalian ESCRT-I and mediates receptor down-regulation. *Mol. Biol. Cell* **15**, 4337-4346.

Bankaitis, V. A., Johnson, L. M. and Emr, S. D. (1986). Isolation of yeast mutants defective in protein targeting to the vacuole. *Proc. Natl. Acad. Sci. USA* **83**, 9075-9079.

Banta, L. M., Robinson, J. S., Klionsky, D. J. and Emr, S. D. (1988). Organelle assembly in yeast: characterization of yeast mutants defective in vacuolar biogenesis and protein sorting. *J. Cell Biol.* **107**, 1369-1383.

Bassham, D. C. and Raikhel, N. V. (2000). Unique features of the plant vacuolar sorting machinery. *Curr. Opin. Cell Biol.* **12**, 491-495.

Bilodeau, P. S., Urbanowski, J. L., Winistorfer, S. C. and Piper, R. C. (2002). The Vps27p Hse1p complex binds ubiquitin and mediates endosomal protein sorting. *Nat. Cell Biol.* **4**, 534-539.

Bilodeau, P. S., Winistorfer, S. C., Kearney, W. R., Robertson, A. D. and Piper, R. C. (2003). Vps27-Hse1 and ESCRT-I complexes cooperate to increase efficiency of sorting ubiquitinated proteins at the endosome. *J. Cell Biol.* **163**, 237-243.

Blum, H., Beier, H. and Gross, H. J. (1987). Improved silver staining of plant proteins, RNA and DNA in polyacrylamide gels. *Electrophoresis* **8**, 93-99.

Carter, R. E. and Sorkin, A. (1998). Endocytosis of functional epidermal growth factor receptor-green fluorescent protein chimera. *J. Biol. Chem.* **273**, 35000-35007.

Downes, B. P., Stupar, R. M., Gingerich, D. J. and Vierstra, R. D. (2003). The HECT ubiquitin-protein ligase (UPL) family in Arabidopsis: UPL3 has a specific role in trichome development. *Plant J.* **35**, 729-742.

Eastman, S. W., Martin-Serrano, J., Chung, W., Zang, T. and Bieniasz, P. D. (2005). Identification of human VPS37C, a component of endosomal sorting complex required for transport-I important for viral budding. *J. Biol. Chem.* **280**, 628-636.

El Refy, A., Perazza, D., Zekraoui, L., Valay, J. G., Bechtold, N., Brown, S., Hulskamp, M., Herzog, M. and Bonneville, J. M. (2004). The Arabidopsis KAKTUS gene encodes a HECT protein and controls the number of endoreduplication cycles. *Mol. Genet. Genomics* **270**, 403-414.

Feng, G. H., Lih, C. J. and Cohen, S. N. (2000). TSG101 protein steady-state level is regulated posttranslationally by an evolutionarily conserved COOH-terminal sequence. *Cancer Res.* **60**, 1736-1741.

Fields, S. and Song, O. (1989). A novel genetic system to detect protein-protein interactions. *Nature* **340**, 245-246.

Galbraith, D. W., Harkins, K. R. and Knapp, S. (1991). Systemic endopolyploidy in *Arabidopsis thaliana*. *Plant Physiol.* **96**, 985-989.

Gietz, R. D., Schiestl, R. H., Willems, A. R. and Woods, R. A. (1995). Studies on the transformation of intact yeast cells by the LiAc/SS-DNA/PEG procedure. *Yeast* **11**, 355-360.

Halladay, J. P. and Craig, E. A. (1996). Genomic Libraries and a host strain designed for highly efficient two-hybrid selection in yeast. *Genetics* **144**, 1425-1436.

Haupt, Y., Maya, R., Kazaz, A. and Oren, M. (1997). Mdm2 promotes the rapid degradation of p53. *Nature* **387**, 296-299.

Hershko, A. (1983). Ubiquitin: roles in protein modification and breakdown. *Cell* **34**, 11-12.

Hofgen, R. and Willmitzer, L. (1990). Biochemical and genetic analysis of different patatin isoforms expressed in various organs of potato (*Solanum tuberosum*). *Plant Sci.* **66**, 221-230.

Hulskamp, M., Misera, S. and Jürgens, G. (1994). Genetic dissection of trichome cell development in *Arabidopsis*. *Cell* **76**, 555-566.

Katzmann, D. J., Babst, M. and Emr, S. D. (2001). Ubiquitin-dependent sorting into the multivesicular body pathway requires the function of a conserved endosomal protein sorting complex, ESCRT-I. *Cell* **106**, 145-155.

Kirik, V., Grini, P. E., Mathur, J., Klinkhammer, I., Adler, K., Bechtold, N., Herzog, M., Bonneville, J. M. and Hulskamp, M. (2002a). The Arabidopsis TUBULIN-FOLDING COFACTOR A gene is involved in the control of the alpha/beta-tubulin monomer balance. *Plant Cell* **14**, 2265-2276.

Kirik, V., Mathur, J., Grini, P. E., Klinkhammer, I., Adler, K., Bechtold, N., Herzog, M., Bonneville, J. M. and Hulskamp, M. (2002b). Functional analysis of the tubulin-folding cofactor C in Arabidopsis thaliana. *Curr. Biol.* **12**, 1519-1523.

Kubbutat, M. H., Jones, S. N. and Vousden, K. H. (1997). Regulation of p53 stability by Mdm2. *Nature* **387**, 299-303.

Laemmli, U. K. (1970). Cleavage of structural proteins during the assembly of the head of bacteriophage T4. *Nature* **227**, 680-685.

Li, L., Liao, J., Ruland, J., Mak, T. W. and Cohen, S. N. (2001). A TSG101/MDM2 regulatory loop modulates MDM2 degradation and MDM2/p53 feedback control. *Proc. Natl. Acad. Sci. USA* **98**, 1619-1624.

Lupas, A., Van Dyke, M. and Stock, J. (1991). Predicting coiled coils from protein sequences. *Science* **252**, 1162-1164.

Magyar, Z., De Veylder, L., Atanassova, A., Bako, L., Inze, D. and Bogre, L. (2005). The role of the Arabidopsis E2FB transcription factor in regulating auxin-dependent cell division. *Plant Cell* **17**, 2527-2541.

Mathur, J. and Koncz, C. (1998). PEG-mediated protoplast transformation with naked DNA. *Methods Mol. Biol.* **82**, 267-276.

Mathur, J., Mathur, N. and Hulskamp, M. (2002). Simultaneous visualization of peroxisomes and cytoskeletal elements reveals actin and not microtubule-based peroxisome motility in plants. *Plant Physiol.* **128**, 1031-1045.

Muller, S., Fuchs, E., Ovecka, M., Wysocka-Diller, J., Benfey, P. N. and Hauser, M. T. (2002). Two new loci, PLEIADE and HYADE, implicate organ-specific regulation of cytokinesis in Arabidopsis. *Plant Physiol.* **130**, 312-324.

Muller, S., Smertenko, A., Wagner, V., Heinrich, M., Hussey, P. J. and Hauser, M. T. (2004). The plant microtubule-associated protein AtMAP65-3/PLE is essential for cytokinetic phragmoplast function. *Curr. Biol.* **14**, 412-417.

Odorizzi, G., Babst, M. and Emr, S. D. (1998). Fab1p PtdIns(3)P 5-kinase function essential for protein sorting in the multivesicular body. *Cell* **95**, 847-858.

Oh, H., Mammucari, C., Nenci, A., Cabodi, S., Cohen, S. N. and Dotto, G. P. (2002). Negative regulation of cell growth and differentiation by TSG101 through association with p21Cip1/WAF1. *Proc. Natl. Acad. Sci. USA* **98**, 5430-5435.

Paris, N., Stanley, C. M., Jones, R. L. and Rogers, J. C. (1996). Plant cells contain two functionally distinct vacuolar compartments. *Cell* **85**, 563-572.

Raymond, C. K., Howald-Stevenson, I., Vater, C. A. and Stevens, T. H. (1992). Morphological classification of the yeast vacuolar protein sorting mutants: evidence for a prevacuolar compartment in class E vps mutants. *Mol. Biol. Cell* **3**, 1389-1402.

Seki, M., Carninci, P., Nishiyama, Y., Hayashizaki, Y. and Shinozaki, K. (1998). High-efficiency cloning of Arabidopsis full-length cDNA by biotinylated CAP trapper. *Plant J.* **15**, 707-720.

Seki, M., Narusaka, M., Kamiya, A., Ishida, J., Satou, M., Sakurai, T., Nakajima, M., Enju, A., Akiyama, K., Oono, Y. et al. (2002). Functional annotation of a full-length Arabidopsis cDNA collection. *Science* **296**, 141-145.

Steinborn, K., Maulbetsch, C., Priester, B., Trautmann, S., Pacher, T., Geiges, B., Kuttner, F., Lepiniec, L., Stierhof, Y.-D., Schwarz, H. et al. (2002). The Arabidopsis PILZ group genes encode tubulin-folding cofactor orthologs required for cell division but not cell growth. *Genes Dev.* **16**, 959-971.

Stuchell, M. D., Garrus, J. E., Muller, B., Stray, K. M., Ghaffarian, S., McKinnon, R., Krausslich, H. G., Morham, S. G. and Sundquist, W. I. (2004). The human endosomal sorting complex required for transport (ESCRT-I) and its role in HIV-1 budding. *J. Biol. Chem.* **279**, 36059-36071.

Swanson, S. J., Bethke, P. C. and Jones, R. L. (1998). Barley aleurone cells contain two types of vacuoles. Characterization of lytic organelles by use of fluorescent probes. *Plant Cell* **10**, 685-698.

Tse, Y. C., Mo, B., Hillmer, S., Zhao, M., Lo, S. W., Robinson, D. G. and Jiang, L. (2004). Identification of multivesicular bodies as prevacuolar compartments in Nicotiana tabacum BY-2 cells. *Plant Cell* **16**, 672-693.

Twell, D., Park, S. K., Hawkins, T. J., Schubert, D., Schmidt, R., Smertenko, A. and Hussey, P. J. (2002). MOR1/GEM1 has an essential role in the plant-specific cytokinetic phragmoplast. *Nat. Cell Biol.* **4**, 711-714.

Ueda, T., Yamaguchi, M., Uchimiya, H. and Nakano, A. (2001). Ara6, a plant-unique novel type Rab GTPase, functions in the endocytic pathway of Arabidopsis thaliana. *EMBO J.* **20**, 4730-4741.

Urbanowski, J. L. and Piper, R. C. (2001). Ubiquitin sorts proteins into the intralumenal degradative compartment of the late-endosome/vacuole. *Traffic* **2**, 622-630.

Verkest, A., Weinl, C., Inze, D., De Veylder, L. and Schnittger, A. (2005). Switching the cell cycle. Kip-related proteins in plant cell cycle control. *Plant Physiol.* **139**, 1099-1106.

Vida, T. A. and Emr, S. D. (1995). New vital stain for visualizing vacuolar membrane dynamics and endocytosis in yeast. *J. Cell Biol.* **128**, 779-792.

Vierstra, R. D. and Callis, J. (1999). Polypeptide tags, ubiquitous modifiers for plant protein regulation. *Plant Mol. Biol.* **41**, 435-442.

Vitale, A. and Raikhel, N. V. (1999). What do proteins need to reach different vacuoles? *Trends Plant Sci.* **4**, 149-155.

Vitale, A. and Galili, G. (2001). The endomembrane system and the problem of protein sorting. *Plant Physiol.* **125**, 115-118.

Winter, V. and Hauser, M. T. (2006). Exploring the ESCRTing machinery in eukaryotes. *Trends Plant Sci.* **11**, 115-123.

Xie, W., Li, L. and Cohen, S. N. (1998). Cell cycle-dependent subcellular localization of the TSG101 protein and mitotic and nuclear abnormalities associated with TSG101 deficiency. *Proc. Natl. Acad. Sci. USA* **95**, 1595-1600.